DNA Sequence and Length Dictate the Assembly of Nucleic Acid Block Copolymers

Felix J. Rizzuto[1,2,3]*, Michael D. Dore[1,3], Muhammad Ghufran Rafique[1], Xin Luo[1] and Hanadi F. Sleiman[1]*

[1]Department of Chemistry, McGill University, 801 Sherbrooke St W, Montréal, QC H3A 08B, Canada

[2]Present address: School of Chemistry, University of New South Wales, Sydney, 2052, Australia

[3]These authors contributed equally.

ABSTRACT: The self-assembly of block copolymers is often rationalized by structure and microphase separation; pathways that diverge from this parameter space may provide new mechanisms of polymer self-assembly. Here, we show that the sequence and length of single-stranded DNA directly influence the self-assembly of sequence-defined DNA block copolymers. While increasing the length of DNA led to predictable changes in self-assembly, changing only the sequence of DNA produced three distinct structures: spherical micelles (spherical nucleic acids, SNAs) from flexible poly(thymine) DNA, fibers from semi-rigid mixed-sequence DNA, and networked superstructures from rigid poly(adenine) DNA. The secondary structure of poly(adenine) DNA strands drives a temperature-dependent polymerization and assembly mechanism: copolymers stored in an SNA reservoir form fibers after thermal activation, which then aggregate upon cooling to form interwoven networks. DNA is often used as a programming code that aids in nanostructure addressability and function; Here, we show that the inherent physical and chemical properties of single-stranded DNA sequences also make them an ideal material to direct self-assembled morphologies and select for new methods of supramolecular polymerization.

Sequence-defined DNA amphiphiles are covalent polymer chains of monodisperse length and specific monomer order attached to single-stranded DNA, constructed efficiently and rapidly on an automated DNA synthesizer.[1-10] Self-assembly arises to minimize contact of the hydrophobic region with water, and the relative volume of the hydrophobic to hydrophilic block can play a major role in determining the assembly morphology.[11-13] Increasing the volume of the hydrophobic phase generally decreases the interfacial curvature (*i.e.*, the curvature of the hydrophobic region at the interface between the two blocks) evolving the morphology from spheres to cylinders to lamellae.[14,15] In the case of DNA block copolymers, this yields supramolecular structures with DNA coronas that can be addressed with functional moieties for numerous biological and materials applications.[7,16-20]

Our group[3,9,21-23] and others[24,25] have explored modulation of the hydrophobic moiety – its size, chemistry and number of repeat monomers – in forming diverse structures, but rarely has altering the hydrophilic DNA chain been investigated as a driving force in self-assembly.[26,27] Single-stranded DNA (ssDNA) chains are not always disordered polymers – electrostatics, π interactions, and base hydrophobicity can alter the conformation, rigidity, and internal structure of ssDNA.[28-33] Furthermore, intramolecular interactions between non-adjacent bases and phosphates on a single strand of DNA may alter chain configuration, even transiently.[34,35] We hypothesized that increasing the local concentration of DNA strands by enforcing their proximity in non-covalent assemblies would organize these otherwise unstable intermolecular interactions, forming structured hydrophilic coronas that directly affect self-assembly behavior.

Here, we investigate the influence of the DNA chain sequence and length in driving the morphology and self-assembly mechanisms of DNA amphiphiles. In line with the assembly principles of microphase separation, we observe that increasing DNA length produces assemblies with greater interfacial curvature. We observe that the sequence of DNA strands plays a significant role in dictating the self-assembled structure. DNA chains of the same length with different sequences produced different products: a random sequence DNA amphiphile was observed to polymerize into fibers over the entire thermal trajectory; one composed of only poly(adenine) residues was sequestered as a spherical micelle and only activated for fiber formation at a specific temperature, and then formed hierarchical aggregates upon cooling; while a third comprised of poly(thymine) was retained as a spherical micelle robustly without fiber formation (Figure 1). The inherent supramolecular chemistries – the persistence length, flexibility, and aromatic interactions – of different sequences of DNA determine the morphology of their resulting assemblies. Increasing the local concentration of these interactions by packing into a polymer corona amplifies these differences, driving the formation of networked superstructures of fibers.

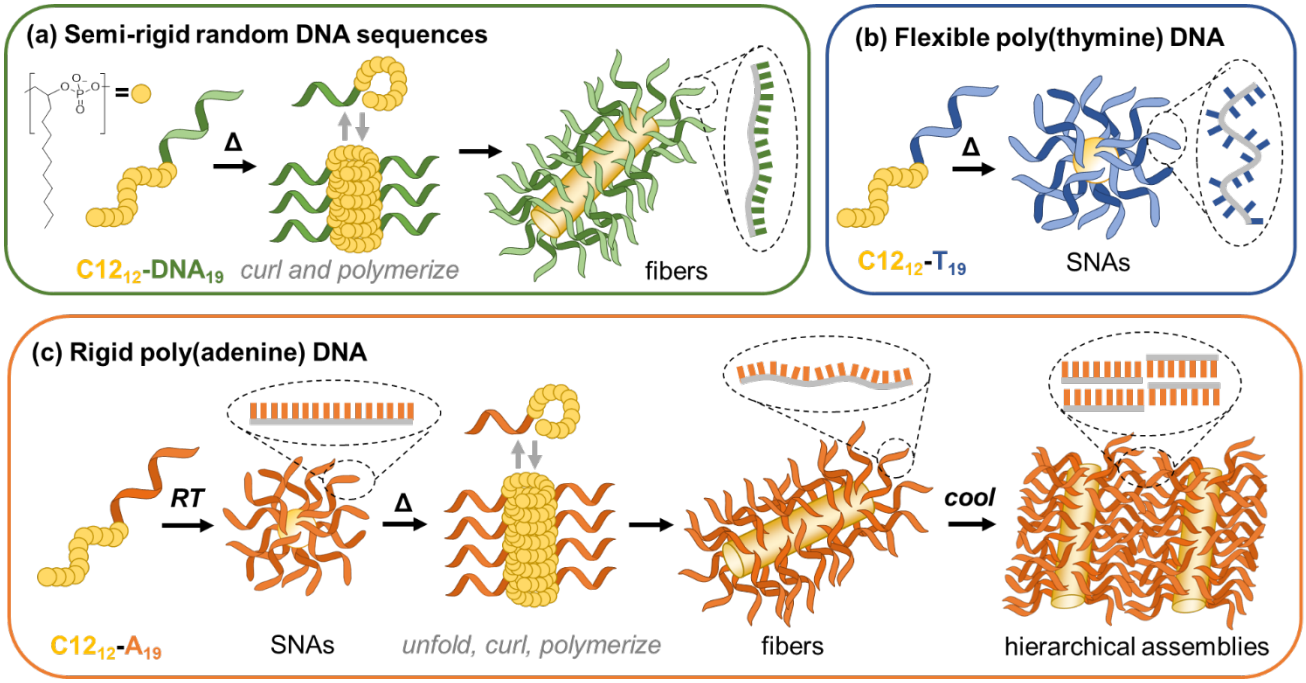

Figure 1. DNA sequence and conformation is a prime determinant in driving amphiphile self-assembly. **(a)** When the DNA is a random sequence (and thus semi-rigid), fiber formation is observed as the hydrophobic tail (yellow) curls during heating; however, **(b)** when the DNA is flexible (polythymine, T_{19}), only SNAs are observed. **(c)** When rigid DNA (polyadenine, A_{19}) is employed, SNAs are initially formed. In this case, the rigidity of the DNA strand prevents polymer reorganization into fibers. Upon heating, the DNA melts to become more flexible, facilitating fiber formation. Upon cooling, the now rigid DNA is capable of blunt end stacking with other fibers. Color code: green – random DNA sequence; blue – poly(thymine); orange – poly(adenine).

RESULTS & DISCUSSION

Changing DNA length

We previously reported a DNA amphiphile containing a covalent polymer with twelve branched hydrophobic monomers (1,2-dodecanediol, **C12**) that are punctuated by phosphates, and appended to a random sequence of 19 DNA bases (**C12$_{12}$-DNA$_{19}$**, Figure 2a). This amphiphile undergoes thermally-driven supramolecular polymerisation to form long, one-dimensional fibers (Figures 1a and 2c):[9] the hydrophobic block curls at elevated temperatures to expose the phosphates and hide the **C12** chains, promoting fusion and fiber elongation (Figure 1a).[9] By increasing the length of the hydrophilic DNA segment, we expect the self-assembly morphology to change following principles of microphase separation: as the amphiphilic packing parameter decreases, we expect assemblies with increasing interfacial curvature.[15] Tuning the relative length of polymer blocks is an efficient tool for controlling

morphology: a size- and shape-defined DNA nanostructure may be assembled from a single molecular species, and each different morphology can influence cellular uptake and bioactivity properties.[36,37]

Lengthening the DNA segment from 19 to 33 bases (**$C12_{12}$-DNA_{33}**) resulted in the formation of spherical nucleic acids (SNAs) (Figure 2d and S8). Dynamic light scattering (DLS) revealed a diffusion coefficient (*D*) an order of magnitude higher and less disperse than the fibres formed by **$C12_{12}$-DNA_{19}** (Table S3), suggesting smaller, more uniform structures that were confirmed by atomic force microscopy (AFM) as SNAs (Figure 2d). Shortening the length of the DNA segment to 5 nucleotide units (**$C12_{12}$-DNA_5**) gave lamellar structures with sheet heights of 7.7 ± 0.5 nm, as observed by AFM (Figures 2b and S9) and reflected in native agarose gel electrophoresis (AGE, Figure S10). DLS gave unstable high intensity signals due to the presence of large aggregated assemblies. We were thus able to switch between three unique polymer morphologies by varying the length of the hydrophilic DNA segment alone from 5 to 33 bases (Figure 2), highlighting the importance of length control in DNA amphiphile self-assembly.

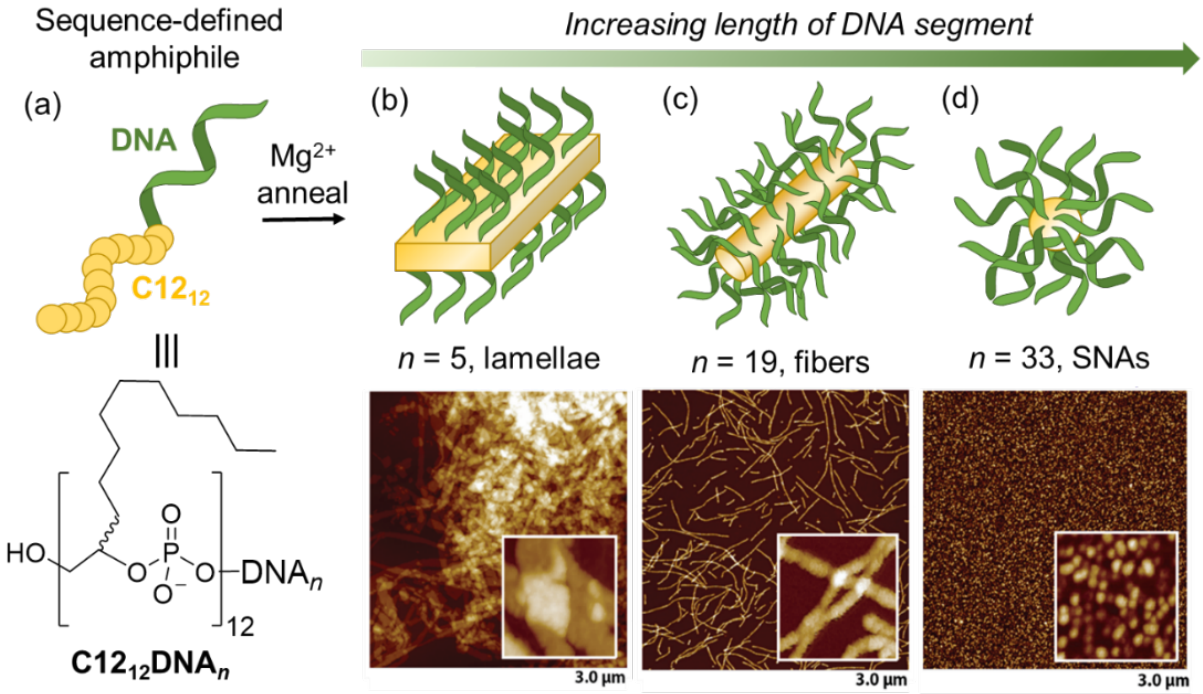

Figure 2. Varying the length of DNA dictates the morphology of resulting self-assembled architectures. **(a)** DNA amphiphiles with 12 C12 units and *n* DNA bases assemble in the presence of Mg^{2+} to form **(b)** lamellae strucutres when *n* = 5, **(c)** fibers when *n* = 19, and **(d)** spherical nucleic acids (SNAs) when *n* = 33, as shown by AFM. Lengths under images indicate width of field of view.

The sequence-specific addressability of the DNA corona allowed us to construct hierarchical superstructures of **C12$_{12}$-DNA$_{19}$** fibers using strand hybridization (Figure 3). When a complement strand **DNA$_{19}$'** was hybridized to fibers of **C12$_{12}$-DNA$_{19}$** in solution, the fiber corona became double stranded. This process produced blunt-ended DNA termini that promoted π-interaction between fibers, resulting in their intermolecular association;[1] Micron-scale hierarchical structures were observed by AFM, composed of densely packed supramolecular fibers aligned parallel to one another (Figures 3a and S11). When a two thymidine overhang was added to **DNA$_{19}$'** and hybridized to fibers of **C12$_{12}$-DNA$_{19}$**, no hierarchical structures were observed, as no blunt ends were available for association (Figure S12). Blunt end stacks can thus be used to control the hierarchical assembly of our addressable DNA fibers. Similar materials are common in biological contexts such as muscle fibers or the extracellular matrix, where organized supramolecular polymers provide mechanical function and specific motifs for interacting with cells.

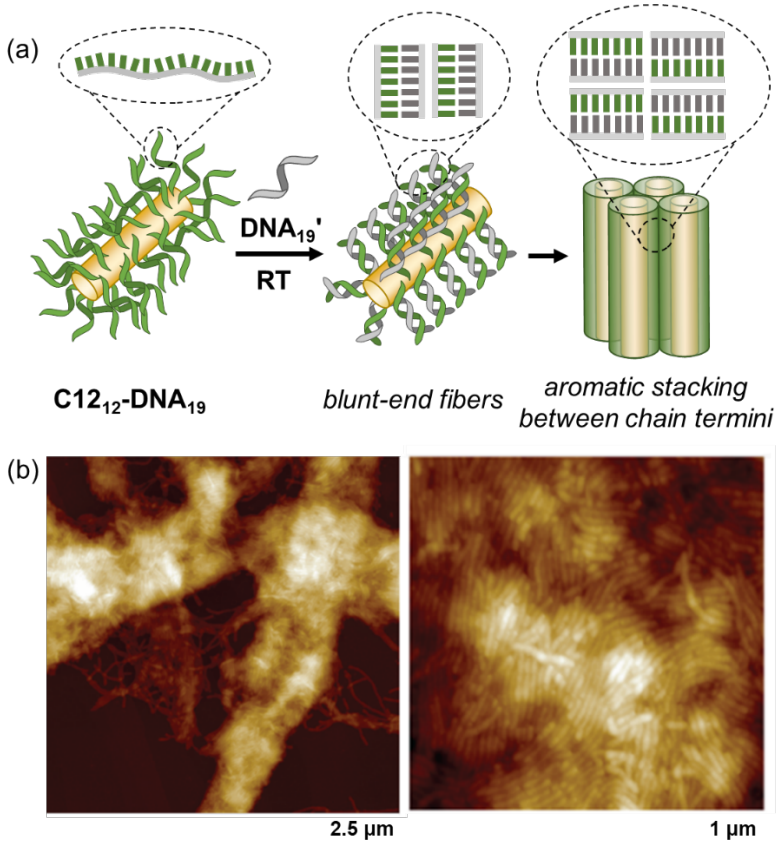

Figure 3. Hierarchical assembly from DNA strand hybridization. (a) When hybridized to a full complement strand **DNA$_{19}$'**, fibers of **C12$_{12}$-DNA$_{19}$** aggregate parallel to one another, forming hierarchical superstructures, **(b)** as observed by AFM.

Changing DNA sequence

We observed that simply changing the sequence of the DNA block, without changing the length of the chain, could alter the self-assembly behavior of our DNA amphiphiles (Figure 1). Our 19mer DNA amphiphile **C12$_{12}$-DNA$_{19}$** was designed as a random sequence with a 5mer thymidine connector proximal to the hydrophobic chains. This amphiphile forms fibers at all annealing temperatures as observed by AGE (Figure S17). Replacing the hydrophilic segment with a 19mer poly(thymine) sequence did not produce fibers when heated up to 90 °C; only spherical micelles were observed by AGE and AFM (Figure 4). In contrast to random DNA sequence **C12$_{12}$-DNA$_{19}$** fibers and **C12$_{12}$-T$_{19}$** spheres, **C12$_{12}$-A$_{19}$** – wherein the DNA sequence is a poly(adenine) – formed SNAs at room temperature, and only formed fibers when annealed above 60 °C (Figure 5 and SI Section 7).

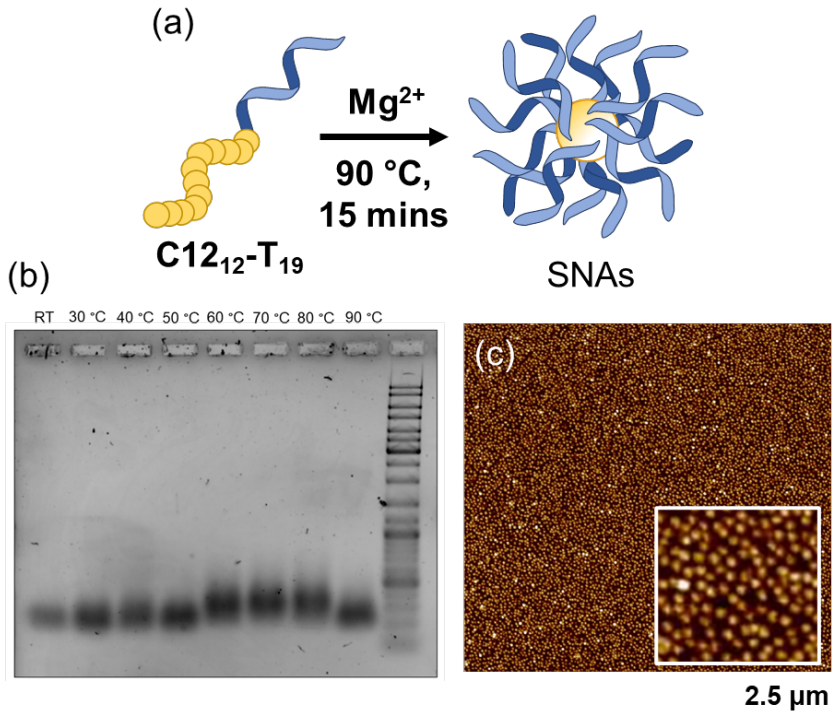

Figure 4. Switching from a random DNA sequence to a poly(thymine) tail forms SNAs, when fibers were predicted. **(a)** **C12$_{12}$-T$_{19}$** forms only SNAs regardless of the heating conditions, as shown by **(b)** native agarose gel electrophoresis (AGE, 1xTAMg buffer). **(c)** AFM of a sample heated to 90 °C. Length under images indicate width of field of view.

These three distinct assembly behaviors – all using the same length of DNA – suggest that the choice of nucleobase affects the amphiphile's self-assembly. The precise structures formed, however, appear counterintuitive: adenine is larger than thymine, such that the volume of a poly(dA) strand

should be larger than that of a poly(dT) strand of equal length, yet we observe assemblies with greater interfacial curvature of poly(dT), as compared poly(dA). Thymidine is also more hydrophobic than adenosine,[28] which should evolve the assembly further, rather than closer, to a spherical morphology. Crucially important, however, is that the persistence length of single-stranded DNA varies greatly with nucleotide number and sequence:[38] for example, a poly(dA) sequence has a higher persistence length than poly(dT), owing to the presence of base stacking interactions between purine bases – it presents as a rigid, structured helix, akin to double-stranded B-DNA.[39-42] We propose that this higher conformational freedom for poly(dT) produces hydrophilic blocks with a larger volume, proximal to the hydrophobic core for **C12$_{12}$-T$_{19}$**; whereas in **C12$_{12}$-A$_{19}$** these hydrophilic DNA blocks are more rigid and elongated, reducing interfacial curvature between blocks and promoting their polymerization. A random DNA sequence – that incorporates a mixture of pyrimidines and purines – has an intermediate persistence length between the extremes of rigid A_{19} (purine only) and flexible T_{19} (pyrimidine only). Despite being all DNA, poly(dA), poly(dT) and a random sequence are analogous to three different hydrophilic polymers with differing rigidity, translating into three unique assembly behaviors.

The polymerization of **C12$_{12}$-A$_{19}$** into fibers was activated abruptly at 60 °C, as discerned by AFM (Figure 5b,c), AGE (Figure 5d) and UV spectra (Figure 5e). By variable temperature UV spectroscopy, we observed the appearance of broad spectral bands at >260 nm past 60 °C, corresponding to the Rayleigh scattering of our thermoset polymers formed *in situ* (Figure S27). Concurrently, we observed a sharp hyperchromicity of the band at 260 nm, accompanied by a decrease in the intensity of all CD bands with increasing temperature (Figure S28). Poly(dA) exists as a structured helix at room temperature;[43] thus our spectroscopic data indicate that stacking interactions between adjacent adenine residues break upon heating, suggesting that the secondary structure of the poly(dA) collapses upon heating and fiber formation. Held rigid and persistent at room temperature, we thus propose that the adenine chains kinetically trap the morphology into a spherical micelle and prevent fiber formation, which requires re-organization and curling of the hydrophobic chains to align on top of one another (Figure 1). At 60 °C, the melting of the adenine stacks brings enough conformational freedom to allow rearrangement of the hydrophobic block and subsequent polymerization into fibrous architectures (Figure 5a).

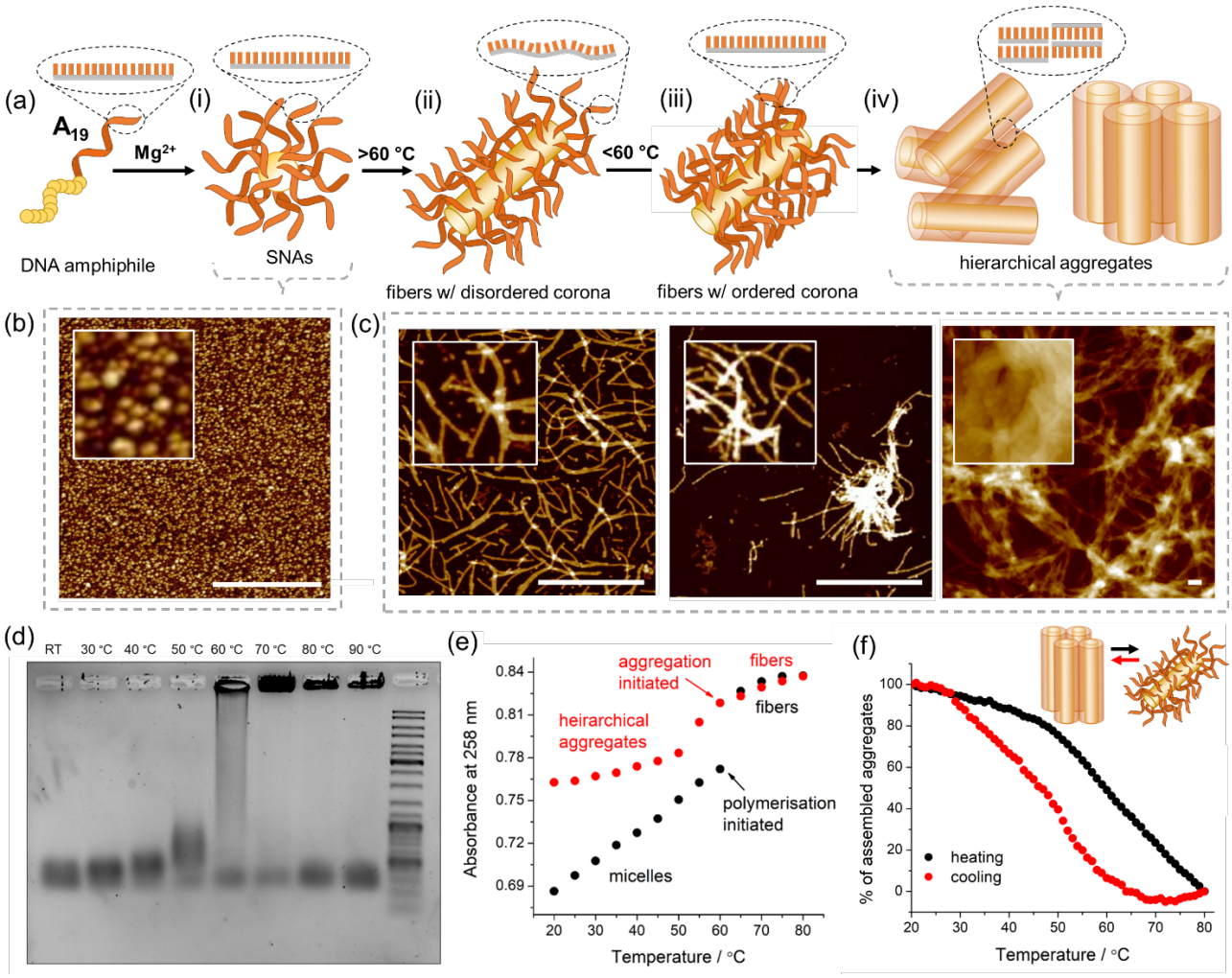

Figure 5. Switching the hydrophilic tail to a poly(dA) sequence forms hierarchical fiber aggregates due to corona dis- and re-ordering. (a) Our DNA amphiphile **C12$_{12}$-A$_{19}$** self-assembles into (i) spherical micelles upon the addition of Mg^{2+}. (ii) Upon heating to 60 °C, fiber polymerization is initiated abruptly. (iii) Upon cooling, the poly(dA) strands behave like structured helices. (iv) The blunt-end termini of these fibers assemble into aggregates. These temperature-activated assemblies are due to conformational differences of the poly(dA) strands, which are shown as cartoon insets throughout (a). **(b)** AFM image of SNAs formed at RT, compared to **(c)** AFM images of different aggregate morphologies observed during rapid cooling (left), as opposed to slow cooling (right). Scale bars are all 1 μm. **(d)** Native AGE (1xTAMg buffer) showing the initiation of polymerization at 60 °C, and the hierarchical aggregates thus formed. **(e)** Variable temperature UV-vis following the absorbance at 258 nm during heating to form our fibers (black) and cooling to form aggregate structures (red). **(f)** These aggregates melt over a broad temperature range starting at 45 °C, and reform with a hysteresis of *ca.* 14 °C, as measured by UV-vis spectroscopy. This melting graph is similar to that observed for poly(dA) strands without hydrophobic attachments (Figure S32).

Upon cooling, our **C12$_{12}$-A$_{19}$** fibers aggregate into hierarchical superstructures (Figure 5), whereas **C12$_{12}$-DNA$_{19}$** is observed as individual long fibers by AFM.[9] The assembly of **C12$_{12}$-A$_{19}$** into superstructures occurs upon cooling in the range 60-50 °C, as shown by hypochromicity in the UV-vis spectra (Figure 5e). The rate of cooling was observed to significantly affect the resulting morphology: Single fibers, two or three fibers in parallel, and starburst fiber structures resulted from rapid cooling (50 °C min^{-1}), whereas slow cooling at 0.2 °C min^{-1} resulted in large, interwoven, and threaded architectures, as observed by AFM (Figure 5c). Commensurate with a slow re-assembly mechanism, a large hysteresis (*ca.* 14 °C) was observed between assembly and disassembly of these superstructures by UV-vis spectroscopy (Figure 5f). The morphology of these superstructures suggest that the DNA corona is directing self-assembly upon cooling.

We hypothesize that both our temperature-specific polymerization and hierarchical aggregates for **C12$_{12}$-A$_{19}$** are a result of the adenine-adenine interactions within and between the DNA chains. Unique among the DNA bases, poly(adenine) strands exist as structured helices in solution, owing to nucleobase high aromatic surface areas, penchant for π-π stacking and self-complementary hydrogen-bonding.[32,39] These interactions break apart upon heating, which may lead to less structured DNA coronas that allow the conversion of kinetically trapped SNAs into fibers (Figure 5ai-ii). Upon cooling, these intramolecular interactions are restabilized: Extended π surfaces form at the corona-solvent boundary from a combination of the rigid, π-stacked individual poly(dA) strands and dynamic blunt-end termini between DNA strands, resulting in superstructures (Figure 5aiii-iv) in a similar manner to the double-stranded blunt-end amphiphile in Figure 5a. The increased local concentration of poly(dA) strands within the fiber coronas may enhance interchain association by hydrogen-bonding (adenine is self-complementary) and/or π -stacking, generating analogous parallel structures with dynamic blunt-end termini.

Single-stranded poly(adenine) DNA is mostly in the C2'-endo or B-DNA form, with a minor contribution of the C3'-endo or A-DNA form.[32,44] The largest contributor to the A-form in a typical d(A)$_n$ strand is the 3'-end residue which has the greatest conformational mobility, as compared to the more rigid internal adenines and 5'-end. In the circular dichroism (CD) spectrum of poly(dA), a positive band at 270 nm indicates the B- vs. A-DNA ratio: the smaller it is, the lower the A-DNA contribution.[44] Thus, the CD band at 270 nm can also indicate the extent of conformational mobility of the 3'-end – the smaller the band, the more rigid the 3'-end, resulting in a lower A-DNA contribution. Upon assembly of **C12$_{12}$-A$_{19}$** into the SNA and fiber states, the positive CD band at 270

nm diminishes, suggesting that, in these nanostructures, the adenine chains are more B-DNA-like (Figure S29). This supports reduced conformational mobility of the 3'-end of poly(dA) sequences in the nanostructures, which lie at the corona-water interface. This more rigid interface in the SNA state can provide an energy barrier to chain rearrangement and fiber formation that is absent in other DNA sequences of the same length. Once the fibers are formed, this rigid corona-solvent interface can result in stronger blunt-end interactions and fiber aggregation.

When a complementary DNA strand with a 2T overhang was hybridized to fibers of **C12$_{12}$-DNA$_{19}$**, we observed that no inter-fiber aggregation occurred (Figure S12). To further investigate our hypothesis of adenine-adenine base stacking interactions in **C12$_{12}$-A$_{19}$**, we capped the 3' terminus of the A$_{19}$ strand with two thymidine monomers (**C12$_{12}$-A$_{19}$T$_2$**). Polymerization to form fibers occurred over all temperature ranges as observed by AGE (Figure S35) without the formation of kinetically trapped SNAs. Fibers were significantly shorter that those of **C12$_{12}$-A$_{19}$** and few hierarchical aggregates were observed by AFM (Figure S36) suggesting that the presence of adenine nucleobases at the solvent-corona boundary was critical for temperature-activated polymerization. It is possible that the 2T overhang folds back onto the A$_{19}$ strands, thus reducing adenine-adenine interactions and decreasing strand rigidity at the 3'-strand ends, which reside the solvent-corona boundary. That **C12$_{12}$-A$_{19}$T$_2$** does not form aggregate superstructures akin to **C12$_{12}$-A$_{19}$** further suggests that blunt-end stacking, rather than inter-fiber hybridization, is responsible for their hierarchical assembly.

We further explored the rigidity of our DNA constructs by adding Hoechst's dye 33342 (Figure 6), a small molecule known to bind to the minor groove of double-stranded DNA, producing a positive included CD (ICD) signal at *ca.* 360 nm.[45] In both the SNA and fiber states of **C12$_{12}$-A$_{19}$** this ICD signal was enhanced as compared to free A$_{19}$, suggesting improved binding of the dye in these assembled states (Figure 6a). In contrast, no ICD signal for **C12$_{12}$-T$_{19}$** was observed, consistent with the greater rigidity and B-DNA character of **C12$_{12}$-A$_{19}$** (Figure 6b). Upon heating the **C12$_{12}$-A$_{19}$** SNAs, the ICD spectrum shifted from one dominated by inter-dye charge transfer (20 → 40 °C), to one dominated by off-resonance dye-DNA exciton coupling (40 → 60 °C), and finally unbinding of the dye (at >60 °C) (Figure S30).[46] These spectral progressions indicate conformational changes occurring in the poly(dA) corona upon heating. Held rigid in the SNA state, the DNA strands melt upon heating, breaking intramolecular adenine-adenine interactions that disorganize the SNA corona, leading to unbinding of the dye as the DNA strand approaches a less structured state.

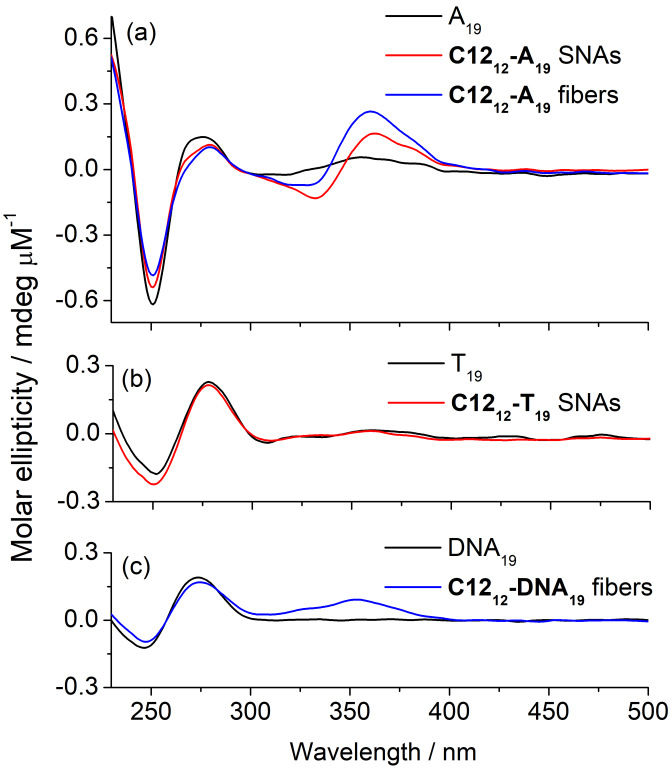

Figure 6. CD spectra of ssDNA and corresponding assemblies with $C12_{12}$ appended, all in the presence of Hoescht's dye (where single stranded DNA is black, SNAs are red and fibers are blue). (a) ssA_{19} DNA compared to **$C12_{12}$-A_{19}** SNAs and fibers; (b) ssT_{19} DNA compared to **$C12_{12}$-T_{19}** SNAs; and (c) $ssDNA_{19}$ compared to **$C12_{12}$-DNA_{19}** fibers. Notably, only assemblies from (a) and (c) showed evidence of interactions with the dye.

Our data suggest that our **$C12_{12}$-A_{19}** SNAs act as reservoirs that firstly store single amphiphile chains and subsequently release them for polymerization following DNA melting. Two forces compete at elevated temperature: As the poly(dA) corona becomes less structured, the thermosetting core cements at the same time. When the corona becomes more dynamic at higher temperature, rearrangement of the hydrophobic strands to a curled conformation is enabled, promoting core fusion and fiber formation. The SNA corona thus provides an additional activation barrier to polymerisation. Increasing temperature overcomes the π-stacking of poly(adenine) strands, allowing their conformations to approximate that of random DNA at elevated temperatures, enabling fiber formation (Figure 5a).

This polymerization mechanism can override the morphology predicted by microphase separation. A 30mer of poly(dA) attached to twelve C_{12} units **$C12_{12}$-A_{30}** formed firstly SNAs at room temperature, followed by the formation of fibers upon heating past 70 °C (Figure 7 and S39), in the same manner

as **C12$_{12}$-A$_{19}$**. This activation temperature is slightly higher than that for the shorter A$_{19}$ sequence, commensurate with the greater degree of thermal stability expected for longer lengths of DNA. **C12$_{12}$-A$_{30}$** fibers also formed hierarchical aggregates depending on their length and rate of cooling. Longer fibers produced micron-length clumpy aggregates when cooled rapidly; they formed extended aggregates when cooled slowly (Figure 7, right). We expected an A$_{30}$ corona to produce SNAs exclusively (in line with the assembly of the random sequence 33mer **C12$_{12}$-DNA$_{33}$** shown in Figure 2). The deviation from an SNA structure at elevated temperature is commensurate with the thermal activation of the DNA strands for fiber formation; upon cooling, the corresponding increase in rigidity of the poly(dA) strands reforms the structured poly(A) helices, forming networked aggregates.

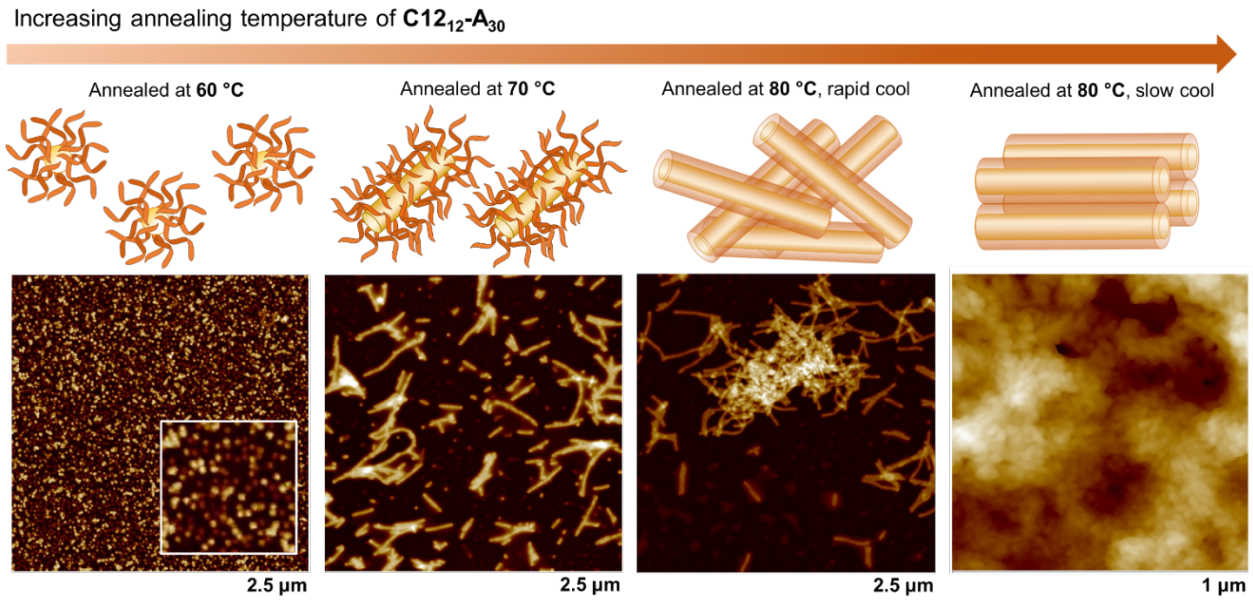

Figure 7. Fiber formation using C12$_{12}$-A$_{30}$ and its hierarchical assembly. **C12$_{12}$-A$_{30}$** polymerized under the same mechanism as **C12$_{12}$-A$_{19}$**, forming spherical micelles up to a specific annealing temperature, over which fibers were formed, which aggregated into superstructures upon cooling. Lengths under images indicate width of field of view.

CONCLUSIONS

The morphology and pathway complexity of self-assembled DNA amphiphiles cannot be predicted by the length of the hydrophilic DNA chain alone. Progressively increasing the *length* of a random sequence DNA block changed the resultant morphology from sheets to fibers to spheres; as expected from changes in the amphiphile packing parameter. In contrast, changing only the *sequence* of DNA had unexpected impacts on the self-assembly. Different morphologies were observed for the same

length of DNA with different sequences – spheres for $\mathbf{T_{19}}$, fibers for random sequence $\mathbf{DNA_{19}}$ and networked fibers for $\mathbf{A_{19}}$ – due to differences in their single-stranded conformations. While fibers were formed at all temperatures for random sequence $\mathbf{DNA_{19}}$ amphiphiles, $\mathbf{A_{19}}$ amphiphiles first assembled into kinetically trapped spherical micelles, and only produced fibers upon thermal denaturation of their structured poly(dA) corona. The assembly pathways were also affected by inter-polymer chain-chain interactions and the solvent-corona interface, driving the assembly of hierarchical superstructures. Resembling biological tissues such as tendon and extracellular matrices, these superstructures consisted of densely packed supramolecular fibers that may find applications in tissue engineering and delivery.

DNA self-assembly in biology and nanotechnology is fundamentally dictated by sequence. In this work we have extended the role of DNA sequence beyond the typical paradigm of complementarity, embracing the chemical and physical properties of specific single-stranded DNA sequences to dictate polymerization and assembly pathways. The results show that different sequences of DNA can act like blocks of different hydrophilic polymers both within, and diverging from, the simple principles of amphiphilic block copolymer self-assembly. The potential to replace other hydrophilic polymers with different sequences of DNA may allow improvements in biocompatibility and therapeutic function of many block copolymer systems. Understanding and developing new corona interactions using DNA amphiphiles could additionally unlock the potential of DNA-minimal structures for new hierarchical assemblies that proffer sensing, diagnostic and drug delivery applications.

ACKNOWLEDGEMENTS

F.J.R. thanks the National Science and Engineering Research Council of Canada (NSERC) for a Banting Fellowship and the Australian Research Council (ARC) for a Discovery Early Career Research Award (DECRA). H.F.S. is thankful to NSERC, the Canada Foundation for Innovation (CFI) and the Fonds de Recherche Nature et Technologies (FRQNT). H.F.S. is also thankful to the Canada Research Chairs Program, the Canada Council for the Arts for a Killam Fellowship and is a Cottrell Scholar of the Research Corporation.

COMPETING INTERESTS STATEMENT

The authors declare no competing interests.

CORRESPONDING AUTHORS

*Felix Rizzuto. Email: f.rizzuto@unsw.edu.au

*Hanadi Sleiman. Email: hanadi.sleiman@mcgill.ca

REFERENCES

1. Vyborna, Y.; Vybornyi, M.; Haner, R., From Ribbons to Networks: Hierarchical Organization of DNA-Grafted Supramolecular Polymers. *J. Am. Chem. Soc.* **2015,** *137* (44), 14051-14054.
2. Nerantzaki, M.; Loth, C.; Lutz, J.-F., Chemical conjugation of nucleic acid aptamers and synthetic polymers. *Polym. Chem.* **2021,** *12* (24), 3498-3509.
3. Edwardson, T.; Carneiro, K.; Serpell, C.; Sleiman, H., An Efficient and Modular Route to Sequence- Defined Polymers Appended to DNA. *Angew. Chem. Int. Ed.* **2014,** *53* (18), 4567-4571.
4. Kwak, M.; Herrmann, A., Nucleic acid amphiphiles: synthesis and self-assembled nanostructures. *Chem. Soc. Rev.* **2011,** *40* (12), 5745-5755.
5. Zhao, Z.; Dong, Y.; Duan, Z.; Jin, D.; Yuan, W.; Liu, D., DNA-organic molecular amphiphiles: Synthesis, self-assembly, and hierarchical aggregates. *Aggregate* **2021,** *2* (4), e95.
6. Lutz, J.-F.; Ouchi, M.; Liu, D. R.; Sawamoto, M., Sequence-Controlled Polymers. *Science* **2013,** *341* (6146), 1238149.
7. Whitfield, C. J.; Zhang, M.; Winterwerber, P.; Wu, Y.; Ng, D. Y. W.; Weil, T., Functional DNA–Polymer Conjugates. *Chem. Rev.* **2021,** *121* (18), 11030-11084.
8. Zhang, C.; Hao, L.; Calabrese, C. M.; Zhou, Y.; Choi, C. H. J.; Xing, H.; Mirkin, C. A., Biodegradable DNA-Brush Block Copolymer Spherical Nucleic Acids Enable Transfection Agent-Free Intracellular Gene Regulation. *Small* **2015,** *11* (40), 5360-5368.
9. Dore, M. D.; Trinh, T.; Zorman, M.; de Rochambeau, D.; Platnich, C. M.; Xu, P.; Luo, X.; Remington, J. M.; Toader, V.; Cosa, G.; Li, J.; Sleiman, H. F., Thermosetting supramolecular polymerization of compartmentalized DNA fibers with stereo sequence and length control. *Chem* **2021,** *9* (9), 2395-2414.
10. Wijnands, S. P. W.; Meijer, E. W.; Merkx, M., DNA-Functionalized Supramolecular Polymers: Dynamic Multicomponent Assemblies with Emergent Properties. *Bioconjug. Chem.* **2019,** *30* (7), 1905-1914.
11. Wang, C.; Wang, Z.; Zhang, X., Amphiphilic Building Blocks for Self-Assembly: From Amphiphiles to Supra-amphiphiles. *Acc. Chem. Res.* **2012,** *45* (4), 608-618.
12. Israelachvili, J. N.; Mitchell, D. J.; Ninham, B. W., Theory of self-assembly of hydrocarbon amphiphiles into micelles and bilayers. *J. Chem. Soc., Faraday Trans. 2* **1976,** *72* (0), 1525-1568.
13. Jia, F.; Li, H.; Chen, R.; Zhang, K., Self-Assembly of DNA-Containing Copolymers. *Bioconj. Chem.* **2019,** *30* (7), 1880-1888.
14. Mai, Y.; Eisenberg, A., Self-assembly of block copolymers. *Chem. Soc. Rev.* **2012,** *41* (18), 5969-5985.
15. Leibler, L., Theory of Microphase Separation in Block Copolymers. *Macromolecules* **1980,** *13* (6), 1602-1617.
16. Averick, S.; Paredes, E.; Li, W.; Matyjaszewski, K.; Das, S. R., Direct DNA Conjugation to Star Polymers for Controlled Reversible Assemblies. *Bioconj. Chem* **2011,** *22* (10), 2030-2037.

17. Alemdaroglu, F. E.; Alemdaroglu, N. C.; Langguth, P.; Herrmann, A., DNA Block Copolymer Micelles – A Combinatorial Tool for Cancer Nanotechnology. *Adv. Mater.* **2008,** *20* (5), 899-902.
18. Lu, X.; Watts, E.; Jia, F.; Tan, X.; Zhang, K., Polycondensation of Polymer Brushes via DNA Hybridization. *J. Am. Chem. Soc.* **2014,** *136* (29), 10214-10217.
19. Li, Z.; Zhang, Y.; Fullhart, P.; Mirkin, C. A., Reversible and Chemically Programmable Micelle Assembly with DNA Block-Copolymer Amphiphiles. *Nano Lett.* **2004,** *4* (6), 1055-1058.
20. Fakih, H. H.; Katolik, A.; Malek-Adamian, E.; Fakhoury, J. J.; Kaviani, S.; Damha, M. J.; Sleiman, H. F., Design and enhanced gene silencing activity of spherical 2′-fluoroarabinose nucleic acids (FANA-SNAs). *Chem. Sci.* **2021,** *12* (8), 2993-3003.
21. Bousmail, D.; Chidchob, P.; Sleiman, H., Cyanine-Mediated DNA Nanofiber Growth with Controlled Dimensionality. *J. Am. Chem. Soc.* **2018,** *140* (30), 9518-9530.
22. Serpell, C. J.; Edwardson, T. G. W.; Chidchob, P.; Carneiro, K. M. M.; Sleiman, H. F., Precision Polymers and 3D DNA Nanostructures: Emergent Assemblies from New Parameter Space. *J. Am. Chem. Soc.* **2014,** *136* (44), 15767-15774.
23. Chidchob, P.; Edwardson, T. G. W.; Serpell, C. J.; Sleiman, H. F., Synergy of Two Assembly Languages in DNA Nanostructures: Self-Assembly of Sequence-Defined Polymers on DNA Cages. *J. Am. Chem. Soc.* **2016,** *138* (13), 4416-4425.
24. Albert, S. K.; Golla, M.; Krishnan, N.; Perumal, D.; Varghese, R., DNA−π Amphiphiles: A Unique Building Block for the Crafting of DNA-Decorated Unilamellar Nanostructures. *Acc. Chem. Res.* **2020,** *53* (11), 2668-2679.
25. Appukutti, N.; Serpell, C., High definition polyphosphoesters: between nucleic acids and plastics. *Polym. Chem.* **2018,** *9* (17), 2210-2226.
26. Liu, H.; Zhu, Z.; Kang, H.; Wu, Y.; Sefan, K.; Tan, W., DNA-Based Micelles: Synthesis, Micellar Properties and Size-Dependent Cell Permeability. *Chem. – Eur. J.* **2010,** *16* (12), 3791-3797.
27. Alemdaroglu, F. E.; Wang, J.; Börsch, M.; Berger, R.; Herrmann, A., Enzymatic Control of the Size of DNA Block Copolymer Nanoparticles. *Angew. Chem. Int. Ed.* **2008,** *47* (5), 974-976.
28. Shih, P.; Pedersen, L. G.; Gibbs, P. R.; Wolfenden, R., Hydrophobicities of the nucleic acid bases: distribution coefficients from water to cyclohexane. *J. Mol. Biol.* **1998,** *280* (3), 421-430.
29. Mignon, P.; Loverix, S.; Steyaert, J.; Geerlings, P., Influence of the π–π interaction on the hydrogen bonding capacity of stacked DNA/RNA bases. *Nucl. Acids Res.* **2005,** *33* (6), 1779-1789.
30. Bosco, A.; Camunas-Soler, J.; Ritort, F., Elastic properties and secondary structure formation of single-stranded DNA at monovalent and divalent salt conditions. *Nucl. Acids Res.* **2013,** *42* (3), 2064-2074.
31. Zhang, Y.; Zhou, H.; Ou-Yang, Z.-C., Stretching Single-Stranded DNA: Interplay of Electrostatic, Base-Pairing, and Base-Pair Stacking Interactions. *Biophys. J.* **2001,** *81* (2), 1133-1143.
32. Gray, D. M.; Ratliff, R. L.; Vaughan, M. R., [19] Circular dichroism spectroscopy of DNA. In *Meth. Enzymol.*, Academic Press: 1992; Vol. 211, pp 389-406.
33. Uzawa, T.; Isoshima, T.; Ito, Y.; Ishimori, K.; Makarov, Dmitrii E.; Plaxco, Kevin W., Sequence and Temperature Dependence of the End-to-End Collision Dynamics of Single-Stranded DNA. *Biophys. J.* **2013,** *104* (11), 2485-2492.
34. Spiegel, J.; Adhikari, S.; Balasubramanian, S., The Structure and Function of DNA G-Quadruplexes. *Trends Chem.* **2020,** *2* (2), 123-136.
35. Abou Assi, H.; Garavís, M.; González, C.; Damha, M. J., i-Motif DNA: structural features and significance to cell biology. *Nucl. Acids Res.* **2018,** *46* (16), 8038-8056.
36. Truong, N. P.; Whittaker, M. R.; Mak, C. W.; Davis, T. P., The importance of nanoparticle shape in cancer drug delivery. *Expert Opin. Drug Deliv.* **2015,** *12* (1), 129-142.

37. Zhao, Z.; Ukidve, A.; Krishnan, V.; Mitragotri, S., Effect of physicochemical and surface properties on in vivo fate of drug nanocarriers. *Adv. Drug Deliv. Rev.* **2019,** *143*, 3-21.
38. Hagerman, P. J., Flexibility of DNA. *Annu. Rev. Biophys.* **1988,** *17* (1), 265-286.
39. Isaksson, J.; Acharya, S.; Barman, J.; Cheruku, P.; Chattopadhyaya, J., Single-Stranded Adenine-Rich DNA and RNA Retain Structural Characteristics of Their Respective Double-Stranded Conformations and Show Directional Differences in Stacking Pattern. *Biochemistry* **2004,** *43* (51), 15996-16010.
40. Sim, A. Y. L.; Lipfert, J.; Herschlag, D.; Doniach, S., Salt dependence of the radius of gyration and flexibility of single-stranded DNA in solution probed by small-angle x-ray scattering. *Phys. Rev. E* **2012,** *86* (2), 021901.
41. Mills, J. B.; Vacano, E.; Hagerman, P. J., Flexibility of single-stranded DNA: use of gapped duplex helices to determine the persistence lengths of Poly(dT) and Poly(dA). *J. Mol. Biol.* **1999,** *285* (1), 245-257.
42. Ke, C.; Humeniuk, M.; S-Gracz, H.; Marszalek, P. E., Direct Measurements of Base Stacking Interactions in DNA by Single-Molecule Atomic-Force Spectroscopy. *Phys. Rev. Lett.* **2007,** *99* (1), 018302.
43. Chakraborty, S.; Sharma, S.; Maiti, P. K.; Krishnan, Y., The poly dA helix: a new structural motif for high performance DNA-based molecular switches. *Nucl. Acids. Res.* **2009,** *37* (9), 2810-2817.
44. Olsthoorn, C. S. M.; Bostelaar, L. J.; De Rooij, J. F. M.; Van Boom, J. H.; Altona, C., Circular Dichroism Study of Stacking Properties of Oligodeoxyadenylates and Polydeoxyadenylate. *Eur. J. Biochem.* **1981,** *115* (2), 309-321.
45. Bucevičius, J.; Lukinavičius, G.; Gerasimaitė, R., The Use of Hoechst Dyes for DNA Staining and Beyond. *Chemosensors* **2018,** *6* (2), 18.
46. Holmgaard List, N.; Knoops, J.; Rubio-Magnieto, J.; Idé, J.; Beljonne, D.; Norman, P.; Surin, M.; Linares, M., Origin of DNA-Induced Circular Dichroism in a Minor-Groove Binder. *J. Am. Chem. Soc.* **2017,** *139* (42), 14947-14953.

TOC Graphic